ResearchGate

See discussions, stats, and author profiles for this publication at: https://www.researchgate.net/publication/243659448

Energetics and Dynamics of Intermolecular Proton-Transfer Processes. 2. Ab Initio Direct Dynamics Calculations of the Reaction H 3 O + + NH 3 → NH 4 + + H 2 O

ARTICLE *in* THE JOURNAL OF PHYSICAL CHEMISTRY · SEPTEMBER 1996

Impact Factor: 2.78 · DOI: 10.1021/jp960943b

CITATIONS
30

READS
10

4 AUTHORS, INCLUDING:

Trygve Ulf Helgaker
University of Oslo
360 PUBLICATIONS **17,218** CITATIONS
SEE PROFILE

Kenneth Ruud
University of Tromsoe
341 PUBLICATIONS **8,517** CITATIONS
SEE PROFILE

Einar Uggerud
Royal Adelaide Hospital
155 PUBLICATIONS **1,980** CITATIONS
SEE PROFILE

Available from: Trygve Ulf Helgaker
Retrieved on: 16 January 2016

Energetics and Dynamics of Intermolecular Proton-Transfer Processes. 2. Ab Initio Direct Dynamics Calculations of the Reaction $H_3O^+ + NH_3 \rightarrow NH_4^+ + H_2O$

Heinz-Hermann Bueker, Trygve Helgaker, Kenneth Ruud, and Einar Uggerud*

Department of Chemistry, University of Oslo, P.O. Box 1033 Blindern, N-0315 Oslo, Norway

Received: March 29, 1996; In Final Form: June 28, 1996[⊗]

Using ab initio direct dynamics, selected reaction trajectories were calculated for the title reaction. The lifetime of the intermediate ion−molecule complex formed upon encounter of the reactants depends strongly on their initial relative orientation. When the proton to be transferred is properly lined up between the oxygen and the nitrogen, rapid transfer is observed. This leads to deposition of a high and nonstatistical fraction of the reaction enthalpy into the product ammonium ion. Less favorable initial orientations appear to give a more statistical distribution of the energy. A strong basis set dependence of the dynamics is observed. It is concluded that moderately large basis functions including polarization functions should be used for future dynamical studies. Alternatively, precise analytical surfaces may be used.

Introduction

The internal energy acquired by a protonated molecule BH^+ formed in a proton-transfer reaction, $AH^+ + B \rightarrow A + BH^+$, determines its reactivity in subsequent reactions, for example, in chemical ionization mass spectrometry (CI).[1−5] The reaction enthapy, given by the difference in the proton affinities of A and B, $\Delta H° = PA(A) - PA(B)$, puts an upper bound on the internal energy of the ion BH^+. The aim of this project is to learn more about the factors that determine the deposition of this energy among the products' internal degrees of freedom and thereby the fraction ending up in the ion BH^+. Theoretical treatments of the dynamics of proton-transfer reactions are sparse in the literature.[6]

In the first paper (paper 1) in this series, we investigated the potential energy surface of the proton-transfer reaction (1) and the structures of the reactants, products, and intermediate complex by ab initio methods.[7]

$$H_3O^+ + NH_3 \rightarrow [H_2O\cdots{}^+HNH_3] \rightarrow H_2O + NH_4^+ \quad (1)$$

With the MP2/6-31G(d,p) wave function, the heat of reaction was calculated to be $\Delta H° = -164$ kJ mol^{-1}. The only minimum along the reaction coordinate, corresponding to the intermediate productlike complex, was found to have an enthalpy of 259 kJ mol^{-1} below that of the reactants. Both results are in excellent agreement with experiment. In addition, paper 1 provides good insight into the potential energy surface of the reaction, giving a two-dimensional representation of the reaction valley region. The present paper is an extension of this study and is concerned with the dynamics of the reaction.

The detailed motion of the individual atoms during the course of a reaction and thus the energy partitioning in the products at the end of the trajectory (when reaction has occurred and the products have separated) depend critically on two factors: (i) the choice of initial conditions (relative velocity of the two reactants, their relative orientation, and their internal energies) and (ii) the forces acting between the atoms.[8−10] In addition to these factors, the numerical accuracy of the method is of key importance. Ideally, one would prefer to perform a large number of complete trajectory calculations sampling a random (e.g., a Boltzmann-type) distribution of initial conditions in accordance with the experimental situation. Each trajectory should be calculated using a potential energy function, $V(\boldsymbol{q})$, that describes the interatomic forces to the highest possible precision. This is best achieved by deriving it from an ab initio wave function that incorporates large atomic basis sets and treatment of electron correlation. However, practical limitations hinder achievement of this ideal goal. Even the calculation of one single ab initio trajectory for this simple reaction turns out to be highly demanding. Because of a tendency for this reaction to form long-lived intermediate reaction complexes, we can at present perform only a limited number of trajectory calculations. On the other hand, carefully chosen trajectories may give valuable information and provide a solid basis for further studies.

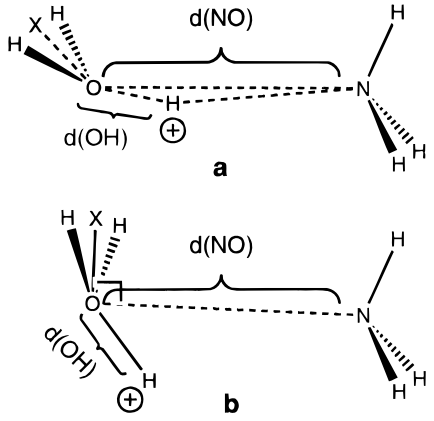

Figure 1. Geometrical structures of the initial configurations chosen for trajectories A−C (a) and trajectory D (b). See the text for a more detailed explanation.

To explore the importance of different initial conditions and levels of ab initio theory, the following four trajectories were calculated: trajectory A, HF/6-31G(d,p), with an initial separation of the reactants H_3O^+ and NH_3 with $d(N-O) = 5.0$ Å (Figure 1a); trajectory B, HF/3-21G, with an initial separation of the reactants H_3O^+ and NH_3 with $d(N-O) = 5.0$ Å; trajectory C, HF/3-21G, with an initial separation of the reactants H_3O^+ and NH_3 with $d(N-O) = 8.0$ Å; trajectory D, HF/3-21G, with an initial separation of the reactants H_3O^+ and NH_3 with $d(N-O) = 5.0$ Å. In the case of trajectory D, the O−H bond does not point toward the nitrogen atom as in the previous calculations. Instead, the H_2O plane of H_2O-H^+ is set to be perpendicular to the N−O line (Figure 1b). For all trajectories,

[⊗] Abstract published in *Advance ACS Abstracts,* August 15, 1996.

S0022-3654(96)00943-4 CCC: $12.00 © 1996 American Chemical Society

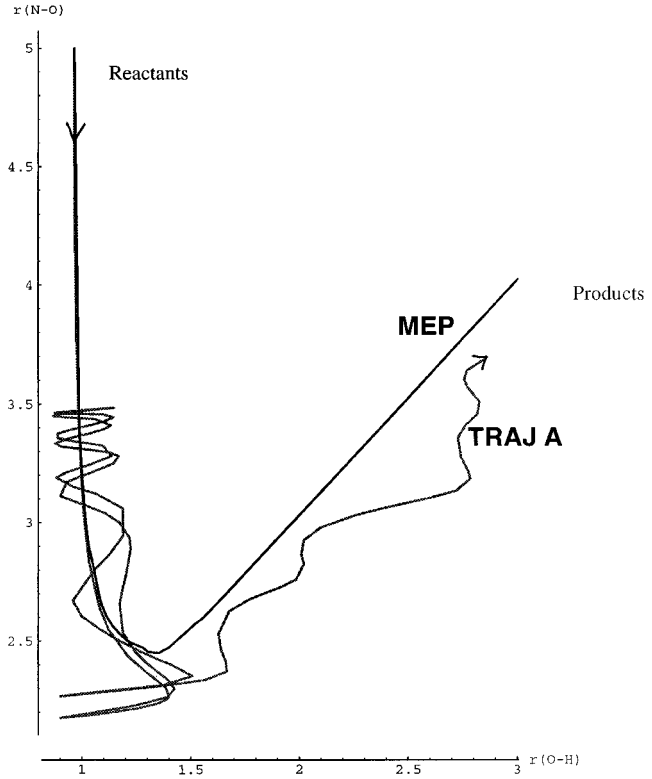

Figure 2. Two-dimensional plot of the minimum energy path (valley bottom) and trajectory A. The minimum energy path is the hyperbolic curve labeled MEP and the trajectory is labeled TRAJ A. The reaction starts in the upper left corner and proceeds as indicated with arrows.

all geometrical parameters (except d(N−O) and in trajectory D also one orientation angle) of the initial configuration were optimized.

In our previous study, MP2/6-31G(d,p) and HF/6-31G(d,p) were found to give very similar potential energy surfaces, whereas HF/3-21G differs slightly (within 10% in the relative energies). Thus, for this reaction, HF/6-31G(d,p) is expected to be as reliable as MP2/6-31G(d,p) but less expensive. HF/3-21G is less accurate but more suitable for a larger number of trajectories or for very long trajectories.

Method of Calculation

During the last decade, efficient algorithms for direct integration of the classical trajectories on ab initio potential energy surfaces have been developed.[11−15] Our ab initio approach uses first and second derivatives (with respect to atomic displacements) of the wave function.[13] One trajectory, $\boldsymbol{q}(t) = \{\boldsymbol{q}_1(t_1), \boldsymbol{q}_2(t_2), ...\}$, is calculated by a stepwise procedure, requiring the recalculation of the wave function at discrete points $\boldsymbol{q}_i$ separated in time typically between 0.1 and 1.0 fs. This approach is obviously very demanding, limiting the accuracy of the wave function which can be employed. In the course of this work, it became clear that even apparantly simple reactions such as the proton-transfer reaction (1) may take place on a time scale of 1 ps or longer. This requires the calculation of 10 000 or more points for 1 single trajectory. The calculations were done at 0 K without inclusion of zero-point vibrational energy. Initial relative orientations of the reactant molecules were chosen as described in the text.

Results and Discussion

Dynamical Path A (1137 Points). A two-dimensional presentation of the trajectory calculated at the HF/6-31G(d,p) level, starting from the optimized reactant complex $H_2O{-}H^+{\cdots}NH_3$ at a separation of d(N−O) = 5.0 Å, is given in Figure 2 in terms of the two geometrical parameters d(N−O) and d(O−H). Figure 3 shows snapshots of the system at critical points

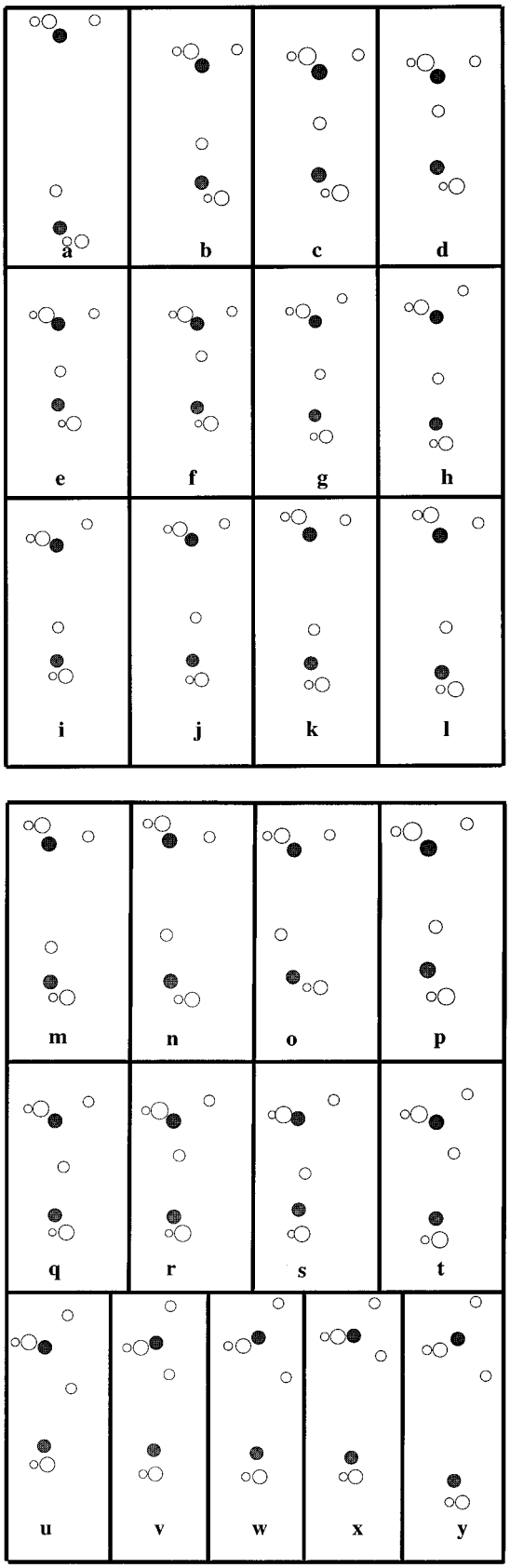

Figure 3. Selected "snapshots" of the instantaneous molecular geometry along trajectory A. The letters a−y refer to the corresponding points marked in Table 1.

TABLE 1: Data from the Dynamical HF/6-31G(d,p) Calculations Starting from the Optimized $H_3N\cdots HOH_2^+$ Complex at $d(NO) = 5.0$ Å (Path A)

iteration no.[a]	accum. time, fs	d(NO), Å	d(OH), Å	d(NH), Å	d(CM),[b] Å	v,[b] km/s
0 (a)	0.0	5.000	0.965	4.042	5.055	0.0
70	92.1	3.990	0.972	3.019	4.050	2.65
120 (b)	119	3.029	1.009	2.019	3.086	4.79
150 (c)	130	2.437	1.211	1.226	2.490	5.94
177 (d)	134	2.254	1.389	0.865	2.292	3.55
205 (e)	139	2.176	0.902	1.277	2.226	0.22
225 (f)	143	2.264	1.395	0.882	2.311	3.73
250	148	2.453	1.246	1.237	2.498	4.90
260 (g)	152	2.659	1.174	1.500	2.711	4.82
270 (h)	157	2.887	1.224	1.664	2.923	3.63
295 (i)	163	3.112	0.902	2.211	*c*	*c*
318 (j)	170	3.280	1.170	2.118	*c*	*c*
337 (k)	176	3.335	0.879	2.463	*c*	*c*
355 (l)	180	3.410	1.134	2.290	*c*	*c*
375 (m)	185	3.450	0.869	2.582	*c*	*c*
403 (n)	190	3.485	1.147	2.343	3.527	0.09
422	195	3.463	0.877	2.597	3.515	0.45
443	201	3.445	1.146	2.320	3.478	0.94
465	206	3.357	0.889	2.503	3.411	1.45
485 (o)	212	3.280	1.136	2.214	3.317	2.01
503	216	3.190	0.884	2.324	3.229	2.38
530	224	2.944	1.190	1.757	2.993	3.57
547 (p)	230	2.671	0.959	1.736	2.758	4.36
565 (q)	236	2.452	1.277	1.214	2.499	4.79
590 (r)	238	2.352	1.509	0.860	2.374	3.45
615	241	2.293	1.192	1.117	2.328	0.51
625 (s)	244	2.268	0.919	1.376	2.323	0.06
665 (t)	251	2.372	1.667	0.879	*d*	*d*
685 (u)	255	2.530	1.629	1.259	*d*	*d*
710 (v)	261	2.759	1.985	0.881	*2.821*	*3.90*
735 (w)	266	2.978	2.100	1.260	*3.013*	*3.72*
755 (x)	271	3.134	2.722	0.871	*3.205*	*3.54*
835 (y)	287	3.682	2.844	1.214	*3.712*	*2.99*
892	300	4.000	3.385	0.917	*4.086*	*2.66*
1137	344	5.000	3.804	1.201	*5.050*	*1.84*

[a] The letters in parentheses correspond to the pictures in Figure 3. [b] Distances of centers of mass d(CM) (Å) and relative velocities v (km/s) refer to the subunits either of the complex $H_3N\cdots HOH_2^+$ or of $H_3NH^+\cdots OH_2$ (*italic* numbers). [c] Not calculated for the complex $H_3N\cdots HOH_2^+$. [d] Not calculated for the complex $H_3NH\cdots OH_2^+$.

of the reaction path. Some data corresponding to these and other points are presented in Table 1.

It can be seen from Figures 2 and 3 and Table 1 that the proton transfer is not a simple straightforward reaction occurring within a single collision of the reactants, as one perhaps might expect for such an exothermic reaction. Starting from the initial configuration, the molecules H_3O^+ and NH_3 approach each other in an accelerating movement due to a strongly attractive force. During this period, the O−H distance increases continuously. As the potential energy minimum is reached and the relative speed is at a maximum, after 130 fs, the force becomes repulsive and the collison partners bounce together. At the inner turning point of this encounter, after 139 fs, d(N−O) is slightly less than 2.2 Å. The proton to be transferred becomes squeezed between the oxygen and the nitrogen, with d(O−H) = 0.90 Å. As a result of this violent collision, the two moieties separate.

The attractive force is strong, however, and after 190 fs, the moieties reach an outer turning point with d(N−O) = 3.5 Å and begin to approach each other again. During the outward and the preceding inward movement, it is interesting to observe that the proton oscillates between N and O eight times. In this second encounter, the inner turning point (with d(N−O) = 2.268 Å) is reached after a total time of 244 fs. At this point, the proton is permanently attached to the NH_3 unit, and it can be seen from the animation that the NH_4^+ product ion is highly exited, with most of the exitation energy in the H−N vibration of the new bond. The attractive force between the product molecules is no longer sufficiently strong to trap them in a complex, and they separate with a substantial relative translational energy. Analysis of the final situation (Table 2) reveals that most (80%) of the potential energy difference between the reactants and product ends up as internal energy of the product ion NH_4^+.

Dynamical Path B (546 Points). Path B differs from path A in that the calculation was performed with the smaller 3-21G basis set, leading to a trajectory which is different in several aspects. The proton transfer occurs within one single encounter of the two moieties. The inner turning point is reached after 136 fs (d(N−O) = 2.139 Å), and after this, the proton stays with the nitrogen atom for a short while. During the first phase of the outward movement, it jumps back to the oxygen atom, but then returns again (at d(N−O) = 2.4 Å). The proton is now permanently attached to the nitrogen atom, and the products separate with a very high relative velocity. Analysis (Table 2) shows that at the end of the trajectory, the internal energy of NH_4^+ is 57% of that totally available.

Comparison of paths A and B indicates that the distribution between the internal energy and the relative translational energy depends critically on the fine-tuning between the oscillating motion of the proton and the relative motion of N and O. A key factor is probably how precisely the interaction potential O···H···N is reproduced by the two basis sets. Obviously, the larger set should give the most realistic description.

Dynamical Path C (1100 Points). This path differs from path B in that the calculation was started and completed at a larger distance. We were interested to see if this is an important factor in the outcome of the trajectory, because one is able to save much computer time if points at large d(N−O) distances prior and subsequent to the reaction can be omitted. Fortunately, path C is very similar to path B in all respects. Only a rather small difference in the energy distributions is observed (Table 2).

Dynamical Path D (7630 Points). Figure 1b shows the initial configuration, with an X−O–N angle of 90°. For the three previous paths, the starting points were chosen to allow for a near-linear alignment of the hydrogen bond O−H···N, which appears to be ideal for fast proton transfer. In reality, randomly chosen initial conditions allow for any possible orientation, so this calculation should give indications of how the reaction may occur in such cases. Clearly, the effect of the initial relative orientation is substantial. While the reaction occurred after 1 or 2 encounters with an initial near-linear orientation, 25 encounters had occurred when this calculation was terminated. At this point, the lifetime of the complex was about to exceed 1 ps. Table 3 shows how the energy is distributed between the internal degrees of freedom for the outer turning points upon termination of the trajectory. It appears that the system is approaching a quite even energy distribution among all the supersystem's available degrees of freedom. A completely even energy distribution would imply 50% in E_{vib}-(NH_4^+) and 17% in $E_{vib}(H_2O)$. This is to be expected since there is a strong tendency for the energy to dissipate among all the system's internal degrees of freedom upon multiple collisions between the two units.

Conclusions and Further Perspectives

On the basis of this limited study, we present the following tentative conclusions:

(a) The quality of the potential energy surface is a key issue. HF/6-31G(d,p) seems to be a minimum necessity. Progress in computer efficiency is required before it is possible to perform

TABLE 2: Results of the Energy Analysis of the Separated Products (Energies in kJ/mol)

trajectory	$E_{vib}(H_2O)$	$E_{rot,kin}(H_2O)$	$E_{vib}(NH_4^+)$	$E_{rot,kin}(NH_4^+)$	$E_{rot,pot}$[a]	E_{trans}[b]
A 5.0 Å 6-31G(d,p)	12.8(7.8%)	0.2(0.1%)	131.0(79.8%)	3.0(1.8%)	2.0(1.2%)	15.2(7.9%)
B 5.0 Å 3-21G(d,p)	0.4(0.3%)	0.0(0.0%)	83.8(57.1%)	0.0(0.0%)	0.0(0.0%)	62.5(42.6%)
C 8.0 Å 3-21G(d,p)	1.0(0.7%)	0.0(0.0%)	87.3(57.9%)	0.2(0.1%)	0.1(0.1%)	62.2(41.3%)

[a] Refers to the whole complex $H_3NH^+\cdots OH_2$. [b] Sum of translational energies of H_2O and NH_4^+.

TABLE 3: Results of the Energy Analysis of the Product Complexes $H_3NH^+\cdots OH_2$ at the Points of Trajectory D with Maximal Distance *d*(CM) of the Subunits (Energies in kJ/mol)

iteration no.	$E_{vib}(H_2O)$	$E_{rot,kin}(H_2O)$	$E_{vib}(NH_4^+)$	$E_{rot,kin}(NH_4^+)$	$E_{rot,pot}$[a]	E_{trans}[b]	E_{total}[c] (ΔE_{pot}[d])
1140	17.0(10.7%)	1.5(0.9%)	139.6(87.5%)	1.5(0.9%)	0.0	0.0	159.6(157.0)
1950	42.9(20.7%)	4.7(2.3%)	157.5(76.1%)	1.0(0.5%)	0.9(0.5%)	0.0	207.0(201.8)
2967	52.2(20.9%)	53.4(21.4%)	102.1(40.9%)	0.1(0.1%)	41.4(16.6%)	0.6(0.2%)	249.7(245.4)
3551	38.6(15.2%)	1.5(0.6%)	149.7(59.1%)	8.8(3.5%)	54.4(21.5%)	0.5(0.2%)	253.4(249.4)
4490	8.3(3.2%)	58.1(22.6%)	150.0(58.3%)	25.6(10.0%)	12.3(4.8%)	3.0(1.2%)	257.3(254.6)
5068	31.6(12.2%)	71.4(27.6%)	133.2(51.4%)	20.4(7.9%)	2.4(0.9%)	0.0	259.1(252.0)
5675	23.0(9.3%)	63.8(25.8%)	130.7(52.9%)	23.1(9.4%)	3.7(1.5%)	2.9(1.2%)	247.2(240.9)
6186	14.0(5.3%)	30.5(11.5%)	192.4(72.8%)	0.2(0.1%)	26.7(10.1%)	3.3(1.3%)	264.1(261.0)
6629	21.8(8.5%)	23.1(9.1%)	181.8(71.4%)	2.3(0.9%)	25.6(10.1%)	0.0	254.6(251.0)
7114	46.5(18.7%)	0.0	148.6(59.9%)	5.9(2.4%)	46.8(18.9%)	0.2(0.1%)	248.0(240.5)
7630	22.5(9.4%)	20.2(8.5%)	143.5(60.2%)	8.3(3.5%)	43.1(18.1%)	0.8(0.3%)	238.4(230.9)

[a] Refers to the whole complex $H_3NH^+\cdots OH_2$. [b] The sum of translational energies of H_2O and NH_4^+ in a turning point is zero. [c] Sum of all energies E_{vib}, $E_{rot,kin}$, $E_{rot,pot}$, and E_{trans} of the complex. [d] Difference of potential energies of the initial starting reactant complex and the most stable complex $H_3NH^+\cdots OH_2$ at the same *d*(NO) as the complex investigated.

a complete dynamical calculation, allowing for 100−200 very long trajectories with randomly sampled initial configurations. An appealing alternative would be to model the potential energy surface by an analytical expression. This has proven to be successful for S_N2 reactions.[16] We are exploring his possibility, but at the moment, we have not been able to find a suitable expression for modeling the O···H···N part of the potential successfully because the angular dependence is very complex.

(b) Multiple encounters occur between the reaction partners during the lifetime of the complex before the reaction is complete. Within each encounter, the proton oscillates several times between the water and the ammonia molecules. When the initial orientation is favorable, the collision complex is short-lived with only a few encounters, leaving a large fraction of the energy in the NH_4^+ ion. For less favorable initial conditions, the reaction complex becomes long-lived, extending into the picosecond regime. In such cases, the energy distribution becomes statistical. It is not possible to make a clear distinction between these two extreme cases at the present time. The effect of relative rotation and internal energy in the reactants also remains to be investigated. Tachikawa has recently studied several proton-transfer reactions by doing trajectory calculations and concluded that they are composed of two channels: direct and complex.[17] It can be seen that our conclusion in this respect is very similar to Tachikawa's.

Acknowledgment. This study is a part of the EU Project "Fundamental studies in gas-phase ion chemistry and mass spectrometry" (Contract No. CHRX-CT93-0291 (DG 12 COMA)). Computer time was made available by the national initiative TRU financed by the Norwegian Research Council.

Appendix: Analysis of the Energy Distributions

For any point along the trajectory, the molecular system can be described in terms of a two-body system A···B of a neutral species and an ion. The total angular momentum

$$\vec{L} = \vec{L}_A + \vec{L}_B + \vec{L}_{AB} \qquad (1)$$

and the total energy

$$E = E_{kin} + E_{pot} = E_{kin}(A) + E_{kin}(B) + E_{pot} \qquad (2)$$

are always conserved. In (1), $\vec{L}_A$ and $\vec{L}_B$ represent the angular momenta of the bodies A and B in their respective center-of-mass systems, whereas $\vec{L}_{AB}$ is the orbital angular momentum of the whole system A···B around its center of mass. In (2), the kinetic energies $E_{kin}(A)$ and $E_{kin}(B)$ of A and B in the center-of-mass system of A···B (CMS(AB)) can expressed as a sum

$$E_{kin}(A) = E_{kin}^{CM}(A) + E_{vib,kin}(A) + E_{rot,kin}(A) \qquad (3)$$

(with a similar expression for B). Here $E_{kin}^{CM}(A)$ is the kinetic energy of the center-of-mass motion of the whole body A, and $E_{vib,kin}$ and $E_{rot,kin}$ are the "internal" vibrational and the rotational kinetic energies of A relative to the CMS(A). For the motion of A and B as whole particles, eq 4 holds

$$E_{kin}^{CM}(A) + E_{kin}^{CM}(B) = E_t(A) + E_t(B) + E_{rot}(AB) \qquad (4)$$

$E_t(A)$ and $E_t(B)$ are the energies of the relative translational motions of A and B, whereas $E_{rot}(AB)$ is the energy of the rotational motion of the whole system A···B around its center of mass. From eqs 3 and 4, the total kinetic energy of the system can be expressed as

$$E_{kin} = E_t(A) + E_t(B) + E_{rot}(AB) + E_{vib,kin}(A) + E_{rot,kin}(A) + E_{vib,kin}(B) + E_{rot,kin}(B) \qquad (5)$$

The first three terms in eq 5, $E_t(A)$, $E_t(B)$, and $E_{rot}(AB)$, refer to the CMS(AB), the other terms $E_{vib,kin}$ and $E_{rot,kin}$ of A and B to the CMS of A and B, respectively.

The kinetic energy terms E_t, $E_{vib,kin}$, and $E_{rot,kin}$ are calculated for each subunit A and B of the reaction complex by the program used, as well as the potential energy E_{pot} of the whole system.

It is also of interest to know the distribution of the potential energy on the vibrational and rotational motions within the complex. The following approximative separation of the total

potential energy of the complex was made

$$E_{pot}(AB) \cong E^0_{pot}(AB) + \Delta E_{vib,pot}(A) + \Delta E_{vib,pot}(B) + \Delta E_{rot,pot}(AB) \quad (6)$$

where $E^0_{pot}(AB)$ is the potential energy minimum of the complex. The other terms in eq 6 are given by

$$\Delta E_{vib,pot}(A) = E_{pot}(AB) - E_{pot}(A_{relax}B) \quad (7)$$

$$\Delta E_{rot,pot}(AB) = E_{pot}(A_{relax}B_{relax}) - E^0_{pot}(AB) \quad (8)$$

$\Delta E_{vib,pot}(A)$ (eq 7) represents a potential energy term for vibrational deformations of the subunit A (with a corresponding expression for B). $E_{pot}(A_{relax}B)$ is the potential energy of the system after relaxation of the geometry of subunit A, whereas the geometry of B, the distance of the centers of mass, and the rotational orientations of A and B remain unchanged.

$\Delta E_{rot,pot}(AB)$ (eq 8) is a potential energy term due to the deviations of the rotational orientations of the subunits A and B from that in the corresponding most stable complex. $E_{pot}(A_{relax}B_{relax})$ is the potential energy of the system after relaxation of the geometries of both subunits A and B, whereas the distance of the centers of mass and the rotational orientation of A and B remain unchanged.

Of course, the equilibrium positions of the nuclei in each of the geometrically relaxed subunits A and B depend at any time on the geometry of the whole complex A···B, this means on the distance of the centers of mass and on the rotational orientation of A and B. The relaxed geometry of each subunit is also influenced to a smaller extent by the actual positions of the nuclei in the other subunit, which change by vibrations. Therefore, the separated potential energy terms in eq 6 depend at any time on the geometry of the whole complex, which is changing with time. Nevertheless, the results of our calculations show that the accuracy of the separation according to eqs 6−8 usually is very good with an error below 1 kJ/mol.

As a consequence of the dependence of $\Delta E_{pot,vib}$ (eq 7) on the geometry of the whole complex, the sum of the vibrational and the rotational energies $E_{vib} + E_{kin,rot} = E_{kin,vib} + \Delta E_{pot,vib} + E_{kin,rot}$ of each subunit within the complex is not a constant, as it is for an isolated vibrating and rotating unit. However, the subunits at a sufficient distance in a complex can be treated as isolated units, for example, the reaction products in a decaying product complex. Therefore, it is of interest to calculate this sum within the energy analysis of a complex.

According to eqs 6−8, it is necessary to calculate relaxed geometries of the single subunits without changing their orientation within the complex. A possible mathematical procedure for these runs is as follows.

Starting from the initial geometry of a subunit, each single step of the geometry optimization procedure leads to displacements $d\vec{r}_i$ of the atoms from their position before the step. These lead to a rotational displacement of the whole subunit, if the sum expression in eq 9 is different from zero.

$$\vec{L}\, dt = \sum_i m_i \vec{r}_i \times d\vec{r}_i \quad (9)$$

In this case, a formal angular momentum vector $\vec{L}$ is calculated from eq 9, where $dt \neq 0$ is an arbitrary scalar. Then the vector $\vec{\omega}$ is determined as the solution of eq 10, where **I** is the momenta-of-inertia tensor of the subunit

$$\vec{L} = \mathbf{I}\cdot\vec{\omega} \quad (10)$$

A rotational displacement of the whole subunit about the vector $-\omega\, dt$ with the displacements $d\vec{r}_i' = -\vec{r}_i \times \vec{\omega}\, dt$ of the atoms then leads to the old orientation of the subunit so that a geometry optimization step with the overall displacements $d\vec{r}_i + dr_i'$ of the atoms leave the orientation of the whole subunit unchanged.

References and Notes

(1) *Proton-Transfer Reactions*; Caldin, E., Gold, V., Eds.; Chapman and Hall: London, 1975.
(2) Zwier, T. S.; Bierbaum, V. M.; Ellison, G. B.; Leone, S. R. *J. Chem. Phys.* **1980**, *72*, 5426.
(3) Weisshaar, J. C.; Zwier, T. S.; Leone, S. R. *J. Chem. Phys.* **1981**, *75*, 4873.
(4) Bowen, R. D.; Harrison, A. G. *Org. Mass Spectrom.* **1981**, *16*, 159.
(5) Harrison, A. G. *Chemical Ionization Mass Spectrometry*, 2nd ed.; CRC: Boca Raton, FL, 1992.
(6) Lim, K. F.; Brauman, J. I. *J. Chem. Phys.* **1991**, *94*, 7164.
(7) Bueker, H. H.; Uggerud, E. *J. Phys. Chem.* **1995**, *99*, 5945.
(8) Bunker, D. L. *Methods Comput. Phys.* **1971**, *10*, 287.
(9) Bunker, D. L. *Acc. Chem. Res.* **1974**, *7*, 195.
(10) Porter, R. N.; Raff, L. M. In *Dynamics of Molecular Collisions, Part B*; Miller, W. H., Ed.; Plenum: New York, 1976; p 1.
(11) Wang, I. S. Y.; Karplus, M. In *J. Am. Chem. Soc.***1973**, *95*, 8160.
(12) Leforestier, C. *J. Chem. Phys.* **1978**, *68*, 4406.
(13) Helgaker, T.; Uggerud, E.; Jensen, H. J. A. *Chem. Phys. Lett.* **1990**, *173*, 145.
(14) Uggerud, E.; Helgaker, T. U. *J. Am. Chem. Soc.* **1992**, *114*, 4265.
(15) Chen, W.; Hase, W. L.; Schlegel, H. B. *Chem. Phys. Lett.* **1994**, *228*, 436.
(16) Hase, W. L. *Science* **1994**, *266*, 998.
(17) Tachikawa, H. *J. Phys. Chem.* **1995**, *99*, 255.

JP960943B